

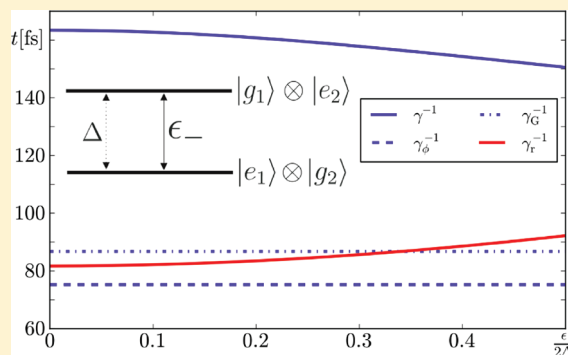
Physical Basis for Long-Lived Electronic Coherence in Photosynthetic Light-Harvesting Systems

Leonardo A. Pachón and Paul Brumer*

Chemical Physics Theory Group, Department of Chemistry and Center for Quantum Information and Quantum Control, University of Toronto, Toronto, Canada M5S 3H6

ABSTRACT: The physical basis for observed long-lived electronic coherence in photosynthetic light-harvesting systems is identified using an analytically soluble model. Three physical features are found to be responsible for their long coherence lifetimes, (i) the small energy gap between excitonic states, (ii) the small ratio of the energy gap to the coupling between excitonic states, and (iii) the fact that the molecular characteristics place the system in an effective low-temperature regime, even at ambient conditions. Using this approach, we obtain decoherence times for a dimer model with FMO parameters of ~ 160 fs at 77 K and ~ 80 fs at 277 K. As such, significant oscillations are found to persist for 600 and 300 fs, respectively, in accord with the experiment and with previous computations. Similar good agreement is found for PC645 at room temperature, with oscillations persisting for 400 fs. The analytic expressions obtained provide direct insight into the parameter dependence of the decoherence time scales.

SECTION: Molecular Structure, Quantum Chemistry, General Theory



Electronic energy transfer is ubiquitous in nature, and its dynamics and manipulation is of special interest in diverse fields of physics, chemistry, biology, and engineering. Under natural conditions, loss of coherence is expected to occur on ultrashort times scale due to interaction with the environment. For example, results on betaine dye molecules¹ and on femto-second dynamics and laser control of charge transport in *trans*-polyacetylene² suggest that these time scales are very short, ~ 2.5 and ~ 3.7 fs, respectively. At high temperatures and for weak coupling to the environment, a classical treatment of the thermal fluctuations suggests that this time scale can be determined as $\tau_G = (\hbar^2/2\lambda k_B T)^{1/2}$, where λ is the system reorganization energy.^{3,4} On the basis of this expression, the dephasing time for photosynthetic complexes, the systems of interest in this paper (wherein a typical value of the reorganization energy is $\lambda = 130$ cm⁻¹), can be estimated⁵ to be $\tau_G = 45$ fs at $T = 77$ K and $\tau_G = 23$ fs and $T = 294$ K.

By contrast, recent experiments in photosynthetic complexes such as the FMO complex^{6,7} and the PC645 complex⁸ have found that electronic coherences among different chromophores survive up to 800 fs at 77 K⁶ and up to 400 fs at room temperature.^{7,8} This surprising observation and its possible consequences for biological processes have been discussed extensively,^{5–16} and very elaborate models have been developed in order to understand the underlying dynamics.^{11,13–16} Interestingly, despite the diversity of approaches and techniques, most^{5,8,10,11,13–16} now predict long-lived coherences on the same times scales as those found experimentally.^{6–8} This suggests that the underlying physical features are correctly contained in these approaches. However, the sheer complexity of these computations

has limited one from identifying these essential physical features.

In this Letter, we present a simple analytic approach that provides deep insights into the long-lived coherences in the evolution of FMO complexes^{5–8,10,11,13,15,16} and PC645^{8,14} and allows for the identification of central characteristics responsible for these long-lived coherences. Our analysis identifies the small effective temperature of the system (see below), the very small, but nonzero, energy gap between exciton states, and their coupling as the basic elements behind these long lifetimes. Given these conditions, we show that the lifetimes are not “surprisingly long”. As such, the challenge now reverts to, for example, obtaining an atomistic understanding¹⁵ of the origins of these parameter values.

Consider first results for the Fenna–Matthews–Olson (FMO) complexes, in particular, the FMO pigment–protein complex from *Chlorobium tepidum*.^{6,7} This is a trimer consisting of identical, weakly interacting monomers.¹⁷ Each weakly interacting FMO monomer contains seven coupled bacteriochlorophyll-*a* (BChl*a*) chromophores arranged asymmetrically, yielding seven nondegenerate, delocalized molecular excited states (excitons).^{6,7} Because the electronic coupling between the BChl*a* 1 and BChl*a* 2 is relatively strong in comparison with the other coupling strengths,¹⁷ we can approximate the dynamics of the excitation as given by a dimer composed by BChl*a* 1 and BChl*a* 2. This, often adopted, approximation is utilized below.

Received: August 29, 2011

Accepted: October 10, 2011

Published: October 10, 2011

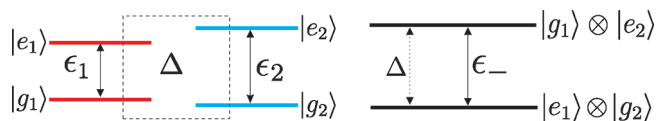


Figure 1. Left-hand side: The pair of interacting chromophores. Right-hand side: the effective light-harvesting two-level system formed from the pair of interacting chromophores.^{19,20}

We consider the dimer (see Figure 1) to be described by the Hamiltonian^{18,19}

$$H = \frac{\hbar}{2}\epsilon_1\sigma_{z,1} + \frac{\hbar}{2}\epsilon_2\sigma_{z,2} + \frac{\hbar}{2}\Delta(\sigma_{x,1}\sigma_{x,2} + \sigma_{y,1}\sigma_{y,2}) + \frac{\hbar}{2}\delta\mu_1\sigma_{z,1}R_1 + \frac{\hbar}{2}\delta\mu_2\sigma_{z,2}R_2 + B_1 + B_2 \quad (1)$$

where $R_i = \sum_{\alpha} C_{\alpha,i}(a_{\alpha,i} + a_{\alpha,i}^{\dagger})$ is the reaction field operator for molecule i , $B_i = \sum_{\alpha} \hbar\omega_{\alpha,i}a_{\alpha,i}^{\dagger}a_{\alpha,i}$ is the energy stored in the solvent cage of molecule i , and $\delta\mu_j$ is the difference between the dipole moment of the chromophore j in the ground and excited states.^{18,19} The first two terms in eq 1 are the contributions from the individual sites, and the third term is the Δ coupling between them. The subsequent terms describe the system–bath coupling. Following refs 19 and 20, the Hamiltonian in eq 1 can be written with respect to the basis $\{|g_1\rangle \otimes |g_2\rangle, |g_1\rangle \otimes |e_2\rangle, |e_1\rangle \otimes |g_2\rangle, |e_1\rangle \otimes |e_2\rangle\}$ describing the state of the two chromophores, that is

$$H = \sum_{i=1,2} \hbar\omega_{\alpha,i}a_{\alpha,i}^{\dagger}a_{\alpha,i} + \frac{\hbar}{2} \begin{pmatrix} -(\epsilon_+ + V_+) & 0 & 0 & 0 \\ 0 & -(\epsilon_- + V_-) & 2\Delta & 0 \\ 0 & 2\Delta & \epsilon_- + V_- & 0 \\ 0 & 0 & 0 & \epsilon_+ + V_+ \end{pmatrix} \quad (2)$$

where $\epsilon_{\pm} \equiv \epsilon_1 \pm \epsilon_2$ and $V_{\pm} \equiv \delta\mu_1R_1 \pm \delta\mu_2R_2$.

Because, under excitation by weak light, only the singly excited states need to be taken into account, we can identify^{19,20} the active environment coupled 2D-subspace as $\{|e_1\rangle \otimes |g_2\rangle, |g_1\rangle \otimes |e_2\rangle\}$. In this central subspace of eq 2, the effective interacting biomolecular two-level system Hamiltonian reads

$$H = \left(\frac{\hbar\epsilon}{2}\sigma_z + \hbar\Delta\sigma_x\right) + \frac{\hbar}{2}\sigma_z V + \sum_{\alpha} \hbar\omega_{\alpha,i}a_{\alpha,i}^{\dagger}a_{\alpha,i} \quad (3)$$

where $\epsilon \equiv \epsilon_-$ and $V \equiv V_-$. This is schematically illustrated in Figure 1, where Δ is the associated “tunneling energy”, between the new basis states $|e_1\rangle \otimes |g_2\rangle$ and $|g_1\rangle \otimes |e_2\rangle$.

Given the biophysical nanostructure composition,¹⁹ we can assume that the two baths are uncorrelated $[a_{\alpha,1}, a_{\alpha,2}^{\dagger}] = 0$, which implies that $\langle R_1(t'')R_2(t') \rangle = \langle R_2(t'')R_1(t') \rangle = 0$. Hence, eq 3 can be written in the standard form of the spin-boson model¹⁹

$$H = \left(\frac{\hbar\epsilon}{2}\sigma_z + \hbar\Delta\sigma_x\right) + \frac{\hbar}{2}\sigma_z \sum_{\beta} g_{\beta}(b_{\beta} + b_{\beta}^{\dagger}) + \sum_{\beta} \hbar\omega_{\beta}b_{\beta}^{\dagger}b_{\beta} \quad (4)$$

Table 1. Parameters Used for the Dimer Formed of BChla 1 and BChla 2 at $T = 77$ (first row) and 277 K (second row)

$\epsilon/2\Delta$	K	$2\Delta/\omega_C$	$2\Delta/k_B T$
0.428	0.105	1.052	3.28
0.428	0.105	1.052	0.911

where the b_{β} includes harmonic oscillators coupled to both chromophores, with couplings g_{β} .

The environment is fully characterized by the spectral density $J(\omega) = \sum_{\alpha} g_{\alpha}^2 \delta(\omega - \omega_{\alpha})$, being a quasi-continuous function for typical condensed-phase applications that determines all bath correlations that are relevant for the system.^{21,22} For Ohmic dissipation, $J(\omega) = 2K\omega e^{-\omega/\omega_C}$, where the dimensionless parameter K describes the damping strength and ω_C is the cutoff frequency.^{21,22} An Ohmic spectral density is a useful choice for, for example, electron-transfer dynamics or biomolecular complexes.^{19,23} The parameter K is related to the reorganization energy λ by means of $\lambda = 2K\hbar\omega_C$, and the phonon relaxation time is given by $\tau = \pi/(2\omega_C)$.^{11,21}

The Hamiltonian in eq 4 has been extensively studied in the literature (cf. Chapters 18–22 in ref 21 and references therein). The parameter range within which the light-harvesting systems of interest lie allows for the use of the non-Markovian noninteracting blip approximation (NIBA) plus first-order corrections in the interblip correlation strength, that is, an enhanced NIBA approximation. This approximation is valid for weak system–bath coupling and for $\epsilon/2\Delta < 1$, over the whole range of temperatures (see Chapter 21 in ref 21), and provides simple and accurate analytic expressions for relaxation and decoherence rates.

In the case of FMO, the energy gap ϵ is $(315 - 240) \text{ cm}^{-1} = 75 \text{ cm}^{-1}$, while the coupling energy Δ corresponds to 87.7 cm^{-1} (see refs 11 and 16 and references therein). In accord with refs 11 and 16, the reorganization energy in this case is $\lambda \approx 35 \text{ cm}^{-1}$, and the phonon relaxation time is $\tau = 50 \text{ fs}$. Hence, for this case, we get $K = \lambda/(2\hbar\omega_C) = \lambda\tau/(\hbar\pi) = 0.105$. Additionally, at $T = 77 \text{ K}$, $2\Delta/k_B T \approx 3.28$, while at $T = 277 \text{ K}$, $2\Delta/k_B T \approx 0.911$. Table 1 summarizes the parameters of the present analysis, where we have used the same ω_C value at both temperatures. Clearly, these parameters place the system within the domain of accuracy of the enhanced NIBA approach. We emphasize that this selection of parameters is widely used in the literature,^{11,16} and it is not chosen to fit our model to the experimental results.

The high-temperature limit in this approach is given by temperatures well in excess of $T_b = \hbar(\Delta_{\text{eff}}^2 + \epsilon^2)^{1/2}/k_B$, where

$$\Delta_{\text{eff}} = [\Gamma(1 - 2K) \cos(\pi K)]^{1/2(1-K)} (\tilde{\Delta}/\omega_C)^{K/(1-K)} \tilde{\Delta}$$

where, in our case, $\tilde{\Delta} = 2\Delta$.

For the set of parameters listed in Table 1, we find $T_b \approx 287 \text{ K}$. Hence, the FMO experiments, at 77 and 277 K, are in the low-temperature regime, $T < T_b$. In this regime, the Rabi frequency Ω , the relaxation rate γ_r and the decoherence rate γ are given by²¹

$$\Omega^2 = \Delta_{\text{eff}}^2 [1 - 2\mathcal{R}u(i\Delta_b)] + \epsilon^2 \quad (5)$$

$$\gamma_r = \frac{\pi}{2} \frac{\Delta_{\text{eff}}^2}{\Delta_b^2} S(\Delta_b) \quad (6)$$

$$\gamma = \frac{\gamma_r}{2} + \frac{\pi K \epsilon^2}{2 \Delta_b^2} S(0) \quad (7)$$

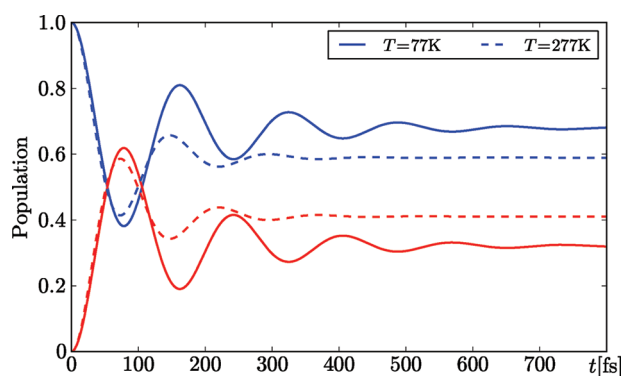


Figure 2. Time evolution of the population of the electronic manifolds $|e_1\rangle\otimes|g_2\rangle|g_2\rangle|e_1\rangle$ (blue curves) and $|g_1\rangle\otimes|e_2\rangle|e_2\rangle|g_1\rangle$ (red curves) for the FMO dimer formed of BChl a 1 and BChl a 2 using the parameters displayed in Table 1. Continuous curves depict the evolution at $T = 77$ K, whereas dashed curves are at $T = 277$ K. We assume that at $t = 0$, the full excitation is localized in $|e_1\rangle\otimes|g_2\rangle|g_2\rangle|e_1\rangle$.

respectively, where $\Delta_b = (\Delta_{\text{eff}}^2 + \varepsilon^2)^{1/2}$ and $u(z) = (1/2) \int_0^\infty d\omega (J(\omega)/(\omega^2 + z^2))(\coth(\hbar\omega/2k_B T) - 1)$ while $S(\omega) = J(\omega) \coth(\hbar\omega/2k_B T)$ is the noise power. Non-Markovian corrections are already included in eqs 5 and 7. For the particular case of Ohmic dissipation adopted here²¹

$$\Omega^2 = \Delta_b^2 + 2K\Delta_{\text{eff}}^2 [\mathcal{R}\psi(i\hbar\Delta_b/2\pi k_B T) - \ln(\hbar\Delta_b/2\pi k_B T)] \quad (8)$$

$$\gamma_r = \pi K \coth(\hbar\Delta_b/2k_B T) \Delta_{\text{eff}}^2 / \Delta_b \quad (9)$$

$$\gamma = \gamma_r/2 + 2\pi K(\varepsilon^2/\Delta_b^2)k_B T/\hbar \quad (10)$$

where $\psi(z)$ is the digamma function. Equations 9 and 10 provide simple analytic expressions for the desired rates.

With this set of expressions, and the parameters given in Table 1, we find $2\pi\Omega^{-1} = 163$ fs, $\gamma_r^{-1} = 90$ fs, and $\gamma^{-1} = 153$ fs at $T = 77$ K, while $2\pi\Omega^{-1} = 151$ fs, $\gamma_r^{-1} = 45$ fs, and $\gamma^{-1} = 69$ fs at $T = 277$ K. Despite the simplicity of the model, the resultant dynamics [given analytically, for general spectral densities, in eqs (21.79), (21.170), and (21.173) of ref 21] is depicted in Figure 2 and describes the survival of coherences on the correct time scale and in good agreement with recent results.^{11,15,16} In Figure 2, only the decay of the excitations is absent because coupling to other chromophores^{11,15,16} is here neglected. The global decay in Figure 2 is a result of two processes, one associated with the γ_r relaxation of the dynamics and a second one related to the loss of coherence due to the presence of the thermal bath, associated with γ .

To examine the parameter dependence, Figure 3 shows the relaxation rate γ_r and the decoherence rate γ as a function of the energy splitting, ε , for fixed Δ , using the parameters displayed in Table 1. Clearly, in this “low-temperature” regime, that is, $T < T_b$, the larger the ratio $\varepsilon/2\Delta$, the shorter the dephasing time and, concomitantly, the longer the relaxation time. These time scales are also compared in Figure 3 with the ones predicted by $\gamma_\phi = 2\pi(k_B T/\hbar)\lambda/\hbar\omega_C$ used in refs 4, 7, and 10 and with $\gamma_G = 1/\tau_G$ discussed earlier, both of which are clearly far too short.

As a second example, we consider results on marine algae,⁵ in particular, the results for PC645, which has been studied experimentally,⁸ and numerically in great detail.¹⁴ PC645 contains

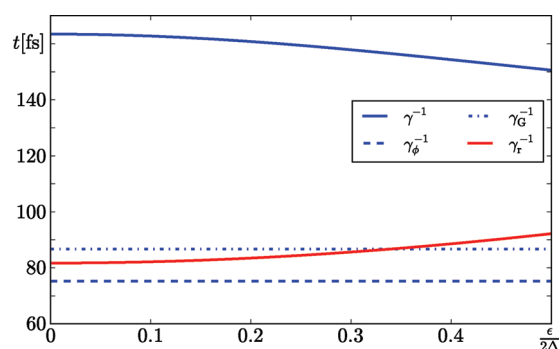


Figure 3. Relaxation time γ_r^{-1} (red line) and decoherence time γ^{-1} (continuous blue line) as functions of $\varepsilon/2\Delta$ for fixed $\Delta = 35$ cm^{−1} and at $T = 77$ K. The dashed blue line, $\gamma_\phi = 2\pi(k_B T/\hbar)\lambda/\hbar\omega_C$, denotes the dephasing rate used in refs 4, 7, and 10, and the dot-dashed blue line denotes the decoherence time $\tau_G = (\hbar^2/2\lambda k_B T)^{1/2}$ used in refs 3–5. Fixed parameters as in Table 1.

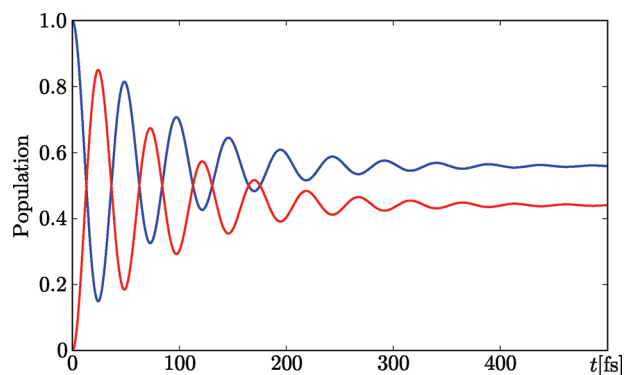


Figure 4. Time evolution of the population of the electronic manifolds $|e_1\rangle\otimes|g_2\rangle|g_2\rangle|e_1\rangle$ (blue curve) and $|g_1\rangle\otimes|e_2\rangle|e_2\rangle|g_1\rangle$ (red curve) for the PC645 DVB dimer.

eight bilin molecules covalently bound to the protein scaffold. A dihydrobiliverdin (DBV) dimer is located at the center of the complex, and two mesobiliverdin (MBV) molecules located near the protein periphery give rise to the upper half of the complex absorption spectrum. Excitation of this dimer initiates the light-harvesting process.⁸ The electronic coupling between the closely spaced DBVc and DBVd molecules is ~ 320 cm^{−1}, and this relatively strong coupling results in delocalization of the excitation, yielding the dimer electronic excited states labeled DBV+ and DBV−. Excitation energy absorbed by the dimer flows to the MBV molecules, which are each 23 Å from the closest DBV, and ultimately to four phycocyanobilins (PCB) that absorb in the lower-energy half of the absorption spectrum.⁸

The exciton states related to DBVc and DBVd are mainly composed of DBV− and DBV+ that are antisymmetric and symmetric linear combinations of the DBV sites, though they also contain small contributions from the other bilin sites.¹⁴ This allows us to concentrate only on a dimer, as in the previous example, here formed of DBVc and DBVd. In this case, a Debye–Ohmic spectral density, $J(\omega) = 2\lambda\omega\tau/(1 + \omega^2\tau^2)$, is more appropriate.¹⁴

For the chromophores DVBc and DVBd, the energy gap is $(17116 - 17034)$ cm^{−1} = 82 cm^{−1}, with the coupling energy corresponding to 319.4 cm^{−1}.^{8,14} In accord with ref 14, the

reorganization energy λ in this case is $\sim 130 \text{ cm}^{-1}$, with the shorter of two relaxation times being $\tau = 50 \text{ fs}$. Additionally, at $T = 294 \text{ K}$, the temperature at which the experiment was performed, $2\Delta/k_{\text{B}}T = 3.1262$. For this set of parameters, we have $T_{\text{b}} \approx 927 \text{ K}$, a high temperature that is consistent with the high frequencies involved in the present case.²⁴ Hence, the PC645 experiment, at room temperature, is also in the effective low-temperature $T < T_{\text{b}}$ domain. For the case of the Debye–Ohmic spectral density, we have (via a relatively simple numerical computation) $2\pi\Omega^{-1} = 49 \text{ fs}$, $\gamma_{\text{r}}^{-1} = 76 \text{ fs}$, and $\gamma^{-1} = 88 \text{ fs}$, with the associated evolution shown in Figure 4. These results are in very good qualitative agreement with both the long-lived experimental coherence time scales and the recent intricate solution to the master equations.¹⁴

Considering that the long time scales emerge naturally here from the system parameters, why were far shorter decoherence time scales originally expected for these systems? To see this, note that in molecular systems, dynamics is often studied between different electronic eigenstates of the system, separated by greater than $\sim 10^4 \text{ cm}^{-1}$, with no coupling between them. In such cases, the dephasing time from eqs 9 and 10 would be extremely short. By contrast, in the case of photosynthetic complexes, energy transfer occurs between exciton states that are close in energy and additionally are coupled. This generates a small value for the ratio ε/Δ , which in turn is responsible for longer dephasing times (see Figure 3). Additionally, expressions such as τ_{G} , which are often used to estimate rates, are only valid at high temperature, $k_{\text{B}}T \gg \hbar\omega_{\text{C}}$, and at short times, $t < \omega_{\text{C}}^{-1}$. Under conditions when the expression for τ_{G} is valid, the bath modes can be treated classically,²⁵ as in refs 1 and 2. When one is not in the appropriate regime, the classical evolution of the bath underestimates quantum coherence effects²⁵ because at low temperatures, quantum fluctuations overcome thermal fluctuations.³ Hence, estimates based on τ_{G} are unreliable. Similarly, $\gamma_{\phi} = 2\pi(k_{\text{B}}T/\hbar)\lambda/\hbar\omega_{\text{C}}$ estimates also provide an inadequate representation of the true physics and associated dependence on system and bath parameters and result in decoherence times that are severely underestimated and misleading.

In summary, a proper spin-boson treatment of electronic energy transfer in model photosynthetic light-harvesting systems has been shown to give analytic results with long coherence lifetimes that are in very good agreement with experiment and with other, far far more complex, computations. The analytic form allows an analysis of the parameter dependence of the decoherence times and shows that the observed long lifetimes arise naturally in the effective low-temperature regime and for appropriate ratios of the energy splitting to the coupling strength and are, in this sense, not surprisingly long. Further, the model has predictive power, allowing one to identify other parameter ranges over which long-lived coherences will exist.

A more detailed analysis will involve extending this model to the seven- or eight-site system and to second-order correction in the interblip approximation; work in this direction is in progress. Finally, in addition to examining other light-harvesting systems, the possible application of this approach to other systems displaying long-lived coherences, such as superpositions of two excitons in quantum dots,²⁶ is of interest.

AUTHOR INFORMATION

Corresponding Author

*E-mail: pbrumer@chem.utoronto.ca.

ACKNOWLEDGMENT

This work was supported by the U.S. Air Force Office of Scientific Research under Contract Number FA9550-10-1-0260.

REFERENCES

- (1) Hwang, H.; Rossky, P. J. Electronic Decoherence Induced by Intramolecular Vibrational Motions in a Betaine Dye Molecule. *J. Phys. Chem. B* **2004**, *108*, 6723–6732.
- (2) Franco, I.; Shapiro, M.; Brumer, P. Femtosecond Dynamics and Laser Control of Charge Transport in Trans-Polyacetylene. *J. Chem. Phys.* **2008**, *128*, 244905.
- (3) Hwang, H.; Rossky, P. J. An Analysis of Electronic Dephasing in the Spin-Boson Model. *J. Chem. Phys.* **2004**, *120*, 11380.
- (4) Gilmore, J. B.; McKenzie, R. H. Quantum Dynamics of Electronic Excitations in Biomolecular Chromophores: Role of the Protein Environment and Solvent. *J. Phys. Chem. A* **2008**, *112*, 2162–2176.
- (5) Cheng, Y.-C.; Fleming, G. R. Dynamics of Light Harvesting in Photosynthesis. *Annu. Rev. Phys. Chem.* **2009**, *60*, 241–262.
- (6) Engel, G. S.; Calhoun, T. R.; Read, E. L.; Ahn, T.-K.; Mančal, T.; Cheng, Y.-C.; Blankenship, R. E.; Fleming, G. R. Evidence for Wavelike Energy Transfer through Quantum Coherence in Photosynthetic Systems. *Nature* **2007**, *446*, 782–786.
- (7) Panitchayangkoon, G.; Hayes, D.; Fransted, K. A.; Carama, J. R.; Harel, E.; Wen, J.; Blankenship, R. E.; Engel, G. S. Long-Lived Quantum Coherence in Photosynthetic Complexes at Physiological Temperature. *Proc. Natl. Acad. Sci. U.S.A.* **2010**, *107*, 12766–12770.
- (8) Collini, E.; Wong, C. Y.; Wilk, K. E.; Curmi, P. M. G.; Brumer, P.; Scholes, G. D. Coherently Wired Light-Harvesting in Photosynthetic Marine Algae at Ambient Temperature. *Nature* **2010**, *463*, 644–647.
- (9) Plenio, M. B.; Huelga, S. F. Dephasing-Assisted Transport: Quantum Networks and Biomolecules. *New J. Phys.* **2008**, *10*, 113019.
- (10) Rebentrost, P.; Mohseni, M.; Kassal, I.; Lloyd, S.; Aspuru-Guzik, A. Environment-Assisted Quantum Transport. *New J. Phys.* **2009**, *11*, 033003.
- (11) Ishizaki, A.; Fleming, G. R. Theoretical Examination of Quantum Coherence in a Photosynthetic System at Physiological Temperature. *Proc. Natl. Acad. Sci. U.S.A.* **2009**, *106*, 17255–17260.
- (12) Wu, J.; Liu, F.; Shen, Y.; Cao, J.; Silbey, R. J. Efficient Energy Transfer in Light-Harvesting Systems, I: Optimal Temperature, Reorganization Energy and Spatial–Temporal Correlations. *New J. Phys.* **2010**, *12*, 105012.
- (13) Briggs, J. S.; Eisfeld, A. Equivalence of Quantum and Classical Coherence in Electronic Energy Transfer. *Phys. Rev. E* **2011**, *83*, 051911.
- (14) Huo, P.; Coker, D. F. Theoretical Study of Coherent Excitation Energy Transfer in Cryptophyte Phycocyanin 645 at Physiological Temperature. *J. Phys. Chem. Lett.* **2011**, *2*, 825–833.
- (15) Shim, S.; Rebentrost, P.; Valleau, S.; Aspuru-Guzik, A. Microscopic Origin of the Long-Lived Quantum Coherences in the Fenna–Matthew–Olson Complex. **2011**, arXiv: 1104.2943v1.
- (16) Nalbach, P.; Braun, D.; Thorwart, M. How “Quantum” Is the Exciton Dynamics in the Fenna–Matthews–Olson Complex? **2011**, arXiv: 1104.2031v1.
- (17) Adolphs, J.; Renger, T. How Proteins Trigger Excitation Energy Transfer in the FMO Complex of Green Sulfur Bacteria. *Biophys. J.* **2006**, *91*, 2778–2797.
- (18) Gilmore, J. B.; McKenzie, R. H. Spin Boson Models for Quantum Decoherence of Electronic Excitations of Biomolecules and Quantum Dots in a Solvent. *J. Phys.: Condens. Matter* **2005**, *17*, 1735–1746.
- (19) Gilmore, J. B.; McKenzie, R. H. Criteria for Quantum Coherent Transfer of Excitations between Chromophores in a Polar Solvent. *Chem. Phys. Lett.* **2006**, *421*, 266–271.
- (20) Eckel, J.; Reina, J. H.; Thorwart, M. Coherent Control of an Effective Two-Level System in a Non-Markovian Biomolecular Environment. *New J. Phys.* **2009**, *11*, 085001.
- (21) Weiss, U. *Quantum Dissipative Systems*, 3rd ed.; World Scientific: Singapore, 2008.

- (22) Leggett, A. J.; Chakravarty, S.; Dorsey, A. T.; Fisher, M. P. A.; Garg, A.; Zwirger, W. Dynamics of the Dissipative Two-State System. *Rev. Mod. Phys.* **1987**, *59*, 1–85.
- (23) May, V.; Kühn, O. *Charge and Energy Transfer Dynamics in Molecular Systems*; Wiley: Berlin, Germany, 2001.
- (24) Galve, F.; Pachón, L. A.; Zueco, D. Bringing Entanglement to the High Temperature Limit. *Phys. Rev. Lett.* **2010**, *105*, 180501.
- (25) Thoss, M.; Wang, H.; Miller, W. H. Self-Consistent Hybrid Approach for Complex Systems: Application to the Spin-Boson Model with Debye Spectral Density. *J. Chem. Phys.* **2001**, *115*, 2991–3005.
- (26) Habenicht, B. F.; Kamisaka, H.; Yamashita, K.; Prezhdo, O. V. Ab Initio Study of Vibrational Dephasing of Electronic Excitations in Semiconducting Carbon Nanotubes. *Nano Lett.* **2007**, *7*, 3260–3265.